Inorganic Chemistry

ARTICLE

pubs.acs.org/IC

# Thermodynamic, Kinetic, and Mechanistic Study of Oxygen Atom Transfer from Mesityl Nitrile Oxide to Phosphines and to a Terminal Metal Phosphido Complex

Xiaochen Cai,[†] Subhojit Majumdar,[†] George C. Fortman,[†] Luis Manuel Frutos,[‡] Manuel Temprado,[*,‡] Christopher R. Clough,[§] Christopher C. Cummins,[*,§] Meaghan E. Germain,[∥] Taryn Palluccio,[∥] Elena V. Rybak-Akimova,[*,∥] Burjor Captain,[*,†] and Carl D. Hoff[*,†]

[†]Department of Chemistry, University of Miami, 1301 Memorial Drive, Coral Gables Florida 33021, United States

[‡]Department of Physical Chemistry, Universidad de Alcalá, Ctra. Madrid-Barcelona Km. 33,600, Madrid, 28871, Spain

[§]Department of Chemistry, Massachusetts Institute of Technology, 77 Massachusetts Avenue, Cambridge, Massachusetts 02139, United States

[∥]Department of Chemistry, Tufts University, 62 Talbot Avenue, Medford, Massachusetts 02155, United States

Supporting Information

**ABSTRACT:** The enthalpies of oxygen atom transfer (OAT) from mesityl nitrile oxide (MesCNO) to $Me_3P$, $Cy_3P$, $Ph_3P$, and the complex $(Ar[^tBu]N)_3MoP$ (Ar = 3,5-$C_6H_3Me_2$) have been measured by solution calorimetry yielding the following P−O bond dissociation enthalpy estimates in toluene solution (±3 kcal $mol^{-1}$): $Me_3PO$ [138.5], $Cy_3PO$ [137.6], $Ph_3PO$ [132.2], $(Ar[^tBu]N)_3MoPO$ [108.9]. The data for $(Ar[^tBu]N)_3MoPO$ yield an estimate of 60.2 kcal $mol^{-1}$ for dissociation of PO from $(Ar[^tBu]N)_3MoPO$. The mechanism of OAT from MesCNO to $R_3P$ and $(Ar[^tBu]N)_3MoP$ has been investigated by UV−vis and FTIR kinetic studies as well as computationally. Reactivity of $R_3P$ and $(Ar[^tBu]N)_3MoP$ with MesCNO is proposed to occur by nucleophilic attack by the lone pair of electrons on the phosphine or phosphide to the electrophilic C atom of MesCNO forming an adduct rather than direct attack at the terminal O. This mechanism is supported by computational studies. In addition, reaction of the N-heterocyclic carbene SIPr (SIPr = 1,3-bis(diisopropyl)phenylimidazolin-2-ylidene) with MesCNO results in formation of a stable adduct in which the lone pair of the carbene attacks the C atom of MesCNO. The crystal structure of the blue SIPr·MesCNO adduct is reported, and resembles one of the computed structures for attack of the lone pair of electrons of $Me_3P$ on the C atom of MesCNO. Furthermore, this adduct in which the electrophilic C atom of MesCNO is blocked by coordination to the NHC does not undergo OAT with $R_3P$. However, it does undergo rapid OAT with coordinatively unsaturated metal complexes such as $(Ar[^tBu]N)_3V$ since these proceed by attack of the unblocked terminal O site of the SIPr·MesCNO adduct rather than at the blocked C site. OAT from MesCNO to pyridine, tetrahydrothiophene, and $(Ar[^tBu]N)_3MoN$ was found not to proceed in spite of thermochemical favorability.

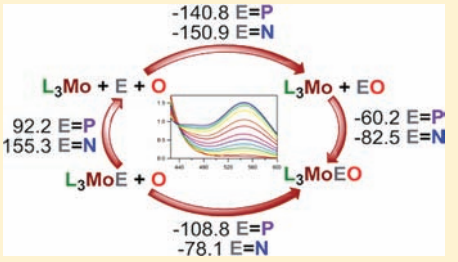


## INTRODUCTION

Oxygen atom transfer (OAT) is a fundamental step in biochemical and industrial oxidative reactions.[1] Selective catalytic oxidation of substrates is at the heart of development of many environmentally benign processes,[2] and understanding the detailed mechanisms of OAT reactions will help in design of such catalysts.

Nitrous oxide is of interest as a green oxidant both because the byproduct of its oxidations is the innocuous $N_2$ molecule, and because it is a thermodynamically powerful oxidant ($D_e$(N−O) ca. 40 kcal $mol^{-1}$).[3] A reality to be dealt with in harnessing $N_2O$ for oxidation chemistry is that it exhibits low reactivity and often can be regarded as essentially an inert gas.[4] Nitrous oxide oxidations may in principle be catalyzed, in furtherance of which coordination complexes of this small molecule have been studied.[5] Recently, an example of such a complex has been characterized in the solid state by X-ray crystallography.[6] A new approach to $N_2O$ chemistry has also emerged in the form of its capture by frustrated Lewis pair (FLP) systems.[7]

Another common class of compounds frequently used in OAT processes is the amine-*N*-oxides. Here as well, transition metal based catalysis of nonmetal oxidations is often required since a number of thermodynamically favorable oxygen atom transfer reactions occur at prohibitively slow rates at room temperature. An example is transfer of an O atom from pyridine-*N*-oxide (PyO) to a phosphine as shown in reaction 1.

(1)

**Received:** June 24, 2011
**Published:** August 29, 2011

 © 2011 American Chemical Society 

In spite of being exothermic by over 70 kcal mol$^{-1}$ because of the strong P═O bond formed, reaction 1 does not occur readily since there is no low energy path available. A simple explanation is that lone pair/lone pair repulsion yields a high energy transition state for this very favorable reaction. This highlights the role kinetic barriers play in oxidative chemistry.[8] Transition metal based catalytic systems have been developed[9] to lower this barrier by the two general steps shown in reactions 2 and 3 which may be representative of a wide range of enzymatic biochemical and catalytic industrial oxidations.

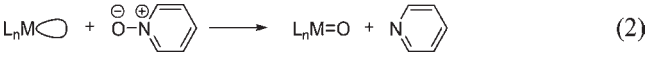

(2)

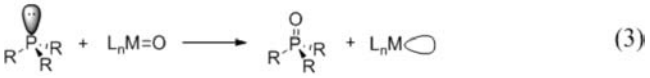

(3)

The step in reaction 2 involves OAT from the oxidant to the metal complex. Espenson and co-workers have recently shown that this requires a vacant coordination site at the metal center to be oxidized.[10] The step in reaction 3 involves OAT from the metal oxide to the substrate. Hall has postulated that this involves attack of the lone pair of the phosphine on an M=O $\pi^*$ orbital.[11] An alternative mechanism involving coupled electron transfer/atom transfer has also been proposed for some OAT steps.[12] The factors controlling the kinetics of reactions 2 and 3 remain an area of great activity. These two steps serve to bracket the M−O bond strength available for a potential catalyst. Ideally this should be stronger than N−O in PyO but weaker than the P═O bond in $R_3PO$. Holm and co-workers have highlighted the importance of a thermodynamic scale for OAT.[13]

Less well appreciated than $N_2O$ and amine-*N*-oxides for OAT reactivity is the class of molecules known as nitrile oxides, RCNO.[14] Like nitrous oxide, the 1,3-dipolar nitrile oxide functional group contains a linear triatomic sequence with a terminal oxygen atom bonded to an *sp* hybridized nitrogen atom. The dative[15] N→O bond distances in substituted benzonitrile oxides are, for example, 1.249(7) and 1.237(10) Å, these being shorter than corresponding distances for trimethylamine-*N*-oxide 1.388 Å or pyridine-*N*-oxide derivatives (1.28−1.30 Å),[16] while longer than that (1.184 Å) in nitrous oxide.[17] The N−O bond dissociation enthalpy (BDE) in MesCNO is only 52.3 kcal mol$^{-1}$, compared to a value of 63.3 kcal mol$^{-1}$ for the N−O BDE in PyO.[18] This makes it a potent OAT reagent thermodynamically, even more so than molecular oxygen itself as implied by the energetics of reaction 4.[19]

$$2\text{MesCNO} \rightarrow 2\text{MesCN} + \text{O}_2 \qquad \Delta H = -14.5\ \text{kcalmol}^{-1} \tag{4}$$

The endothermic nature of $O_2$ addition to MesCN suggests that this reagent may be of value for "difficult" oxidations. Indeed unlike both $N_2O$ and amine-*N*-oxides, nitrile oxides are known to effect the oxidation of tertiary phosphines within minutes upon mixing in solution at room temperature according to reaction 5.[20] The reasons why reaction 1 requires a catalyst and reaction 5 does not have not been delineated.

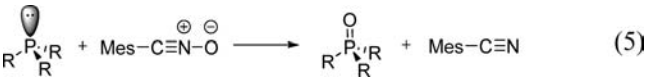

(5)

Furthermore, for conversion of the terminal phosphide complex $(Ar[^tBu]N)_3MoP$ to its oxide, $(Ar[^tBu]N)_3MoPO$, the harsh oxidant dimethyl dioxirane (DMDO) was required, as both $N_2O$ and amine-*N*-oxides failed to react.[21] As described in this report, MesCNO smoothly effects OAT to $(Ar[^tBu]N)_3MoP$, suggesting that this reagent class ought to be considered more generally for OAT processes. In this regard, Beck and co-workers have reported the oxidation of coordinated phosphines by stable nitrile oxides as shown in reaction 6.[22] $Fe(CO)_5$ is capable of deoxygenating nitrile oxides to nitriles in moderate yields.[23]

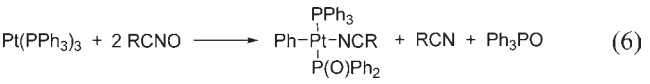

(6)

In spite of these attractive results we have found only limited use of MesCNO in literature reports of OAT reactions. A characteristic organic reaction of nitrile oxides is 1,3-cycloaddition.[24] Likewise, the use of nitrile oxides in cycloaddition reactions of organometallic complexes is well documented.[25]

The work reported here began with an interest in simply utilizing MesCNO as an oxidant in calorimetric studies, first for $R_3P$ to calibrate it for work in solution calorimetry, and then for $(Ar[^tBu]N)_3MoP$ (Ar = 3,5-$C_6H_3Me_2$) to generate data on the Mo−P and P−O bond strengths in the known unique terminal phosphorus monoxide complex $(Ar[^tBu]N)_3MoPO$.[21] This work extends our earlier thermodynamic and kinetic studies of chalcogen atom transfer for E = S, Se, and Te (but not O) for $R_3P$, NHC (NHC = *N*-heterocyclic carbene), $(Ar[^tBu]N)_3MoP$ and $(Ar[^tBu]N)_3Mo$.[26] In our studies of sulfur atom transfer (SAT) to NHCs, $Ph_3SbS$ was utilized as a useful single S atom transfer reagent to NHCs as shown in eq 7.

$$\text{Ph}_3\text{SbS} + \text{SIPr} \rightarrow \text{Ph}_3\text{Sb} + \text{SIPr}{=}\text{S} \tag{7}$$

It was hoped in the current work to extend this to the OAT by using MesCNO as a single O atom transfer reagent for NHCs as shown in eq 8.

$$\text{MesCNO} + \text{SIPr} \not\rightarrow \text{MesCN} + \text{SIPr=O} \tag{8}$$

To our surprise, full oxidation as shown in reaction 8 did not occur. The potential oxidation of the NHC to a cyclic urea stopped at simple adduct formation, and we were able to isolate and structurally characterize the blue SIPr·MesCNO complex in which the lone pair of electrons of SIPr binds to the electropositive C atom of MesCNO. NHC ligands such as SIPr strongly resemble $R_3P$ ligands in their bonding to both metal and nonmetal acids.[27] Isolation of the SIPr·MesCNO adduct led us to postulate that the observed kinetic OAT facility of MesCNO to phosphines might be conferred by initial attack of $R_3P$ at the MesCNO nitrile carbon atom to form an adduct related to that observed in SIPr·MesCNO. That hypothesis was confirmed by detailed computational studies of the reaction profile which are also reported here.

The primary focus of the current work is the energetics and mechanism of oxidation of nonmetals by MesCNO. Limited


dx.doi.org/10.1021/ic2013599 |*Inorg. Chem.* 2011, 50, 9620–9630

preliminary results on reactions of transition metal complexes with MesCNO are reported here to confirm mechanistic ideas regarding these nonmetal reactions. Detailed kinetic and thermodynamic studies of metal complex oxidations by MesCNO will be reported separately.[28]

## EXPERIMENTAL SECTION

Unless stated otherwise, all operations were performed in a Vacuum Atmospheres or MBraun drybox under an atmosphere of purified nitrogen or argon. Diethyl ether and toluene were dried and deoxygenated by the method of Grubbs.[29] $C_6D_6$ was purchased from Cambridge Isotopes. The deuterated solvents were degassed and dried over 4 Å molecular sieves. The 4 Å sieves and Celite were dried in vacuo overnight at a temperature just above 200 °C. Mesityl nitrile oxide was prepared and recrystallized according to the literature.[30] All other compounds were used as received. $^1$H NMR spectra were recorded on a Bruker Avance-400 spectrometer at room temperature. $^1$H NMR chemical shifts are reported in parts per million (ppm) with respect to the protio impurities referenced at 7.16 ppm for $C_6D_6$ and 2.09 ppm for toluene-$d^8$. FTIR spectra were obtained using a Perkin-Elmer Spectrum 400 FTIR Spectrometer. Calorimetric measurements were made using a Setaram C-80 Calvet microcalorimeter.

**Synthesis of (Ar[$^t$Bu]N)$_3$MoPO using MesCNO.** In the glovebox, 299 mg (0.456 mmol) of bright yellow (Ar[$^t$Bu]N)$_3$MoP[21] was dissolved in 5 mL of $CH_2Cl_2$, and the solution was cooled to −35 °C. A solution of MesCNO, 84 mg (1.1 equiv) in 2 mL of $CH_2Cl_2$ (also cooled to −35 °C) was added rapidly to the yellow solution. An additional 1 mL of chilled $CH_2Cl_2$ was used to ensure that all MesCNO had been transferred to the reaction mixture. Upon warming to room temperature, the reaction mixture changed from yellow to deep purple in color. The mixture was stirred for 1 h after mixing to ensure complete reaction. The mixture was then filtered through a bed of Celite, which was washed with 5 mL of chilled $CH_2Cl_2$. The filtrate was then reduced in volume to about 50% of its original volume. The purple reaction mixture was cooled, and 30 mL of thawing acetonitrile was added to precipitate the product. The cold mixture was filtered on a medium-porosity glass frit, and the purple solid was washed with 10 mL of cold acetonitrile. The solid was dried under reduced pressure and yielded (Ar[$^t$Bu]N)$_3$MoPO as a deep purple powder (175 mg, 0.261 mmol, 57%). $^1$H and $^{31}$P NMR data agreed with previously published data.[12]

**Synthesis of the SIPR·MesCNO Adduct.** In the glovebox, 0.400 g of SIPr in 10 mL of toluene was added to 0.1657 g of MesCNO, and the mixture was shaken to dissolve the MesCNO. The solution turned blue-violet, and some solid began to precipitate out. It was left undisturbed in the glovebox overnight. Evaporation of toluene and addition of heptane led to isolation of the pure adduct in 95% yield. Analysis for $C_{37}H_{49}N_3O$: theory (found): C 80.5 (79.2), H 8.9 (8.9), N 7.6 (7.0). The mass spectrum showed a strong peak at 552.39 corresponding to P + 1 for $C_{37}H_{49}N_3O$ = 551.38. $^1$H NMR (400M, $C_6D_6$): $\delta$ = 6.89 (t, 2H, *p*-Ph of SIPr), 6.76 (d, 4H, *m*-Ph of SIPr), 6.45 (s, *m*-Ph of MesCNO), 3.64 (t, 4H, $CH_2$ of SIPr), 3.32 (septet, 4H, CH of $^i$Pr), 2.04 (s, 3H, *p*-$CH_3$ of MesCNO), 1.84 (s, 6H, *o*-$CH_3$ of MesCNO), 1.26 (d, 12H, $CH_3$ of $^i$Pr), 0.95 (d, 12H, $CH_3$ of $^i$Pr) ppm.

**Crystallographic Analyses.** Violet single crystals of SIPr·MesCNO suitable for X-ray diffraction analyses obtained by evaporation of solutions of toluene at 25 °C, crystallized in the monoclinic crystal system. The data crystal was glued onto the end of a thin glass fiber. X-ray intensity data were measured by using a Bruker SMART APEX2 CCD-based diffractometer using Mo K$\alpha$ radiation ($\lambda$ = 0.71073 Å). The raw data frames were integrated with the SAINT+ program by using a narrow-frame integration algorithm.[31] Corrections for Lorentz and polarization effects were also applied with SAINT+. An empirical absorption correction based on the multiple measurement of equivalent reflections was applied using the program SADABS. All structures were solved by a combination of direct methods and difference Fourier syntheses, and refined by full-matrix least-squares on $F^2$, by using the SHELXTL software package.[32] Crystal data, data collection parameters, and results of the analyses are listed in the Supporting Information.

The systematic absences in the intensity data were consistent with the unique space group $P2_1/c$. Half a molecule of toluene from the solvent of crystallization cocrystallized with the complex and is present in the asymmetric crystal unit. The toluene molecule is disordered about an inversion center, and was modeled in part using geometric restraints and refined with isotropic thermal parameters. However, this disorder could not be completely resolved, which resulted in the relatively high *R* value (7.46%). There is not much disorder present in the nonsolvent part of the structure. An ORTEP drawing of the structure is shown in the Results section, see Figure 3. Tables of crystallographic data and the .cif file are available in the Supporting Information.

**Calorimetric Measurement of Reaction of (Ar[$^t$Bu]N)$_3$MoP and R$_3$P with MesCNO.** In the glovebox a solution of 0.5093 g (Ar[$^t$Bu]N)$_3$MoP (0.776 mmol) was dissolved in 6 mL of $C_6D_6$, and 1 mL of this stock solution was loaded into an NMR tube. The remaining 5 mL of solution were loaded into the Calvet calorimeter cell with MesCNO (0.0100 g, 0.062 mmol) as limiting reagent. The calorimeter cell was sealed, taken from the glovebox, and loaded into the Setaram C-80 calorimeter. Following temperature equilibration, the reaction was initiated, and the calorimeter rotated to achieve mixing. Following return to baseline the calorimeter cell was taken into the glovebox, opened, and 1 mL of the solution loaded into an NMR tube. NMR spectra of both the stock solution and the calorimetry solution were then acquired, and the reaction was confirmed as quantitative. The enthalpy of three measurements done in this way led to $\Delta H = -52.3 \pm 0.7$ kcal mol$^{-1}$ based on the reaction (Ar[$^t$Bu]N)$_3$MoP (tol. sol.) + MesCNO (solid) → (Ar[$^t$Bu]N)$_3$MoPO (tol. sol.) + MesCN (tol sol.). To these data the enthalpy of solution of MesCNO in toluene (+4.3 ± 0.1 kcal mol$^{-1}$) was subtracted to give $\Delta H_{rxn}$ = −56.6 ± 0.8 kcal mol$^{-1}$ with all species in toluene solution. Reactions of $R_3P$ were performed in a similar fashion, but typically with five independent measurements on each phosphine.

**UV−vis Kinetic Study of Reaction of (Ar[$^t$Bu]N)$_3$MoP and MesCNO.** Solid (Ar[$^t$Bu]N)$_3$MoP and MesCNO were dissolved in dry dichloromethane or dry toluene under Ar in an MBraun glovebox. The solutions of (Ar[$^t$Bu]N)$_3$MoP were loaded into 1 cm path length airtight quartz cuvettes, and solutions of MesCNO were loaded into Hamilton gastight syringes. Initial spectra of (Ar[$^t$Bu]N)$_3$MoP (0.6 mM) were collected on a JASCO V-570 UV−vis/NIR spectrophotometer, the MesCNO solution was added to the cuvette via syringe, and the reaction was monitored in 1−10 min intervals over a total time of 20−60 min. Variable temperature (15−45 °C) measurements were achieved using the JASCO PSC-498T temperature controller. The kinetic experiments were run under pseudo first order conditions with excess MesCNO (25 mM−100 mM) by monitoring the absorbance increase at $\lambda$ = 550 nm. Data analysis was performed with IGOR pro 5.0 by WaveMetrics.

**FTIR Kinetic Study of the Reaction of MesCNO with R$_3$P, and (Ar[$^t$Bu]N)$_3$MoP.** In the glovebox, a stock solution of MesCNO was prepared (0.125 g in 20 mL of freshly distilled toluene). In a separate vial, 0.100 g of (Ar[$^t$Bu]N)$_3$MoP was dissolved in 2 mL of toluene. A 5 mL syringe was loaded with 4 mL of the MesCNO stock solution, and a 2.5 mL syringe was used to load the 2.0 mL of (Ar[$^t$Bu]N)$_3$MoP in toluene. The 4.0 mL solution was loaded into a thermostatted reaction vessel and allowed to equilibrate with respect to temperature. The 2.0 mL (Ar[$^t$Bu]N)$_3$MoP solution was then injected into the reactor and the timer started. The thermostatted reaction vessel was fitted via thick wall Teflon tubing lines to a thermostatted FTIR cell kept in a temperature and environment controlled chamber. A total of 4.0 mL of solution was flushed under Ar pressure through the tubing and cell through a valve with tubing leading to a vent. The valve was closed so

that under Ar pressure, the thermostatted cell was filled with a solution 0.0258 M in MesCNO and 0.0254 M in $(Ar[^tBu]N)_3MoP$. A series of FTIR spectra were collected of the reaction mixture approximately every 20 s through the first two half-lives, and at a slightly slower rate as the reaction progressed. Data for the nearly equimolar reaction were analyzed by standard techniques and found to obey second order kinetics. Averaged rate data are collected in Table 3 for reactions studied by FTIR spectroscopy.

**Reaction of the SIPr·MesCNO adduct with $(Ar[^tBu]N)_3V$ and $(Ar[^tBu]N)_3Mo$.** In the glovebox, 0.010 g of $(Ar[^tBu]N)_3V$ was dissolved into 1 mL of $C_6D_6$, and this solution was syringed onto 0.0095 g of the blue SIPr·MesCNO adduct in a vial. The mixture was shaken, and there was an immediate change in color to red-orange. The sample was transferred to an NMR tube. Analysis of the NMR spectrum showed complete conversion to MesCN, $(Ar[^tBu]N)_3VO$, and free SIPr. Similar results were obtained using $(Ar[^tBu]N)_3Mo$.

**Attempted Reaction of SIPr·MesCNO and $(Ar[^tBu]N)_3MoP$ and $Cy_3P$.** In the glovebox, 0.0295 g $(Ar[^tBu]N)_3MoP$ was dissolved into 2 mL of $C_6D_6$, and this solution was syringed onto 0.025 g of the blue SIPr·MesCNO adduct in a vial. The mixture was shaken yielding a green solution. The sample was transferred to an NMR tube. Analysis of the NMR spectrum showed no reaction had occurred after a 3 h period. Similar results were obtained in the attempted reaction of SIPr·MesCNO and $Cy_3P$. In this case the solution remained blue in color, and no reaction could be detected by NMR spectroscopy.

**Attempted Reaction of MesCNO and Pyridine, Tetrahydrothiophene and $(Ar[^tBu]N)_3MoN$.** Several reagents were checked qualitatively at room temperature for reactivity with MesCNO. A total of 27.9 mg of MesCNO was dissolved in 1 mL of toluene. To this was added 1 mL of pyridine, and the solution was monitored by FTIR spectroscopy. No decrease in the band due to MesCNO was observed over approximately 4 h. In similar experiments, tetrahydrothiophene and also $(Ar[^tBu]N)_3MoN$ were found to not react at room temperature as followed by NMR and FTIR spectroscopy.

**Computational Details.** Electronic structure calculations were carried out using the B3LYP[33,34] and M05-2X[35] density functionals with the 6-311G(d,p) and 6-311G(3df,2p) basis sets as implemented in the Gaussian 09 suite of programs.[36] Minimum energy and transition state structures were optimized by computing analytical energy gradients. The obtained stationary points were characterized by performing energy second derivatives, confirming them as minima or first order saddle points by the number of negative eigenvalues of the Hessian matrix of the energy (zero and one negative eigenvalues respectively). Computed electronic energies were corrected for zero-point energy, thermal energy, and entropic effects to obtain the corresponding thermodynamic properties $H^0$ and $G^0$. To derive binding energies, the basis set superposition error (BSSE) was computed using counterpoise calculations.[37] For the metal-containing species $(Ar[^tBu]N)_3MoP$ and $(Ar[^tBu]N)_3MoPO$, optimizations were performed using the Stuttgart-Dresden MWB28[38] quasi-relativistic effective core potential and basis including a set of additional f functions for Mo and the triple-ζ quality basis set (6-311G(d,p)) for all other elements.

Intrinsic reaction coordinate (IRC) calculations[39] were done to describe the reaction mechanism for PhCNO and $Me_3P$, providing the connection between the minimum energy points through the different transitions states. Further optimization of the final points of the IRCs with steepest descent algorithm was done to obtain the real minimum energy structures.

Moreover, the energy of the compounds studied was calculated using Gaussian-n theory at the G3 level when applicable.[40] G3 corresponds effectively to calculations at the QCISD(T)/G3large level, G3large being a modification of the 6-311+G(3df,2p) basis set, including more polarization functions for the second row (3d2f), less on the first row (2df), and other changes to improve uniformity. In addition, some core polarization functions are added. Single-point energy calculations are carried out on MP2(full)/6-31G(d) optimized geometries, incorporating scaled HF/6-31G(d) zero-point vibrational energies, a so-called higher-level correction to accommodate remaining deficiencies, and spin−orbit correction for atomic species only.

**Table 1. Enthalpies of Reaction of MesCNO and $A_nP$ in Toluene Solution and Derived P═O BDE Data[a]**

| $A_nP$ | $\Delta H$ | P═O BDE | P═S BDE |
|---|---|---|---|
| $(Ar[^tBu]N)_3MoP$ | $-56.6 \pm 0.8$ | 108.9 | 78 |
| $Ph_3P$ | $-79.9 \pm 1.7$ | 132.2 | 88 |
| $Cy_3P$ | $-85.3 \pm 1.8$ | 137.6 | 98 |
| $Me_3P$ | $-86.2 \pm 1.7$ | 138.5 | 94 |

[a] In kcal $mol^{-1}$. For comparison purposes previously reported P═S data[26] are also included.

## RESULTS

**Reaction of MesCNO and $(Ar[^tBu]N)_3MoP$.** The initial target of this work was improved synthesis and determination of the thermochemistry of the previously characterized purple-blue complex $(Ar[^tBu]N)_3MoPO$.[21] Attempted preparation from PyO as shown in reaction 9 did not occur at room temperature in toluene solution, which is in keeping with the known inability of PyO to oxidize phosphines.

$$(Ar[^tBu]N)_3MoP + PyO \not\longrightarrow (Ar[^tBu]N)_3MoPO + Py \qquad (9)$$

In contrast, reaction of MesCNO with the bright yellow complex $(Ar[^tBu]N)_3MoP$ was found to occur rapidly in toluene solution to yield purple $(Ar[^tBu]N)_3MoPO$ and MesCN in quantitative yield as determined by NMR spectroscopy and shown in reaction 10.

$$(Ar[^tBu]N)_3MoP + MesCNO \rightarrow (Ar[^tBu]N)_3MoPO + MesCN \qquad (10)$$

Previous preparation of $(Ar[^tBu]N)_3MoPO$ involved reaction with dimethyldioxirane at −78 °C. The pathway in reaction 10 provides a more convenient method for in situ generation of $(Ar[^tBu]N)_3MoPO$ and basis for further exploration of its reactivity.[21b]

**Thermochemistry of OAT from MesCNO to $(Ar[^tBu]N)_3MoP$ or $R_3P$.** Solution calorimetric measurements of reactions 5 and 10 were performed in toluene solution at 30 °C using Calvet calorimetry with solid mesityl nitrile oxide as limiting reagent. Values for the enthalpies of reaction with all species in toluene solution are collected in Table 1 together with bond strength estimates and earlier reported data for sulfur atom transfer (SAT).[26] Data on the BDE in toluene solution are considered accurate to ±3 kcal $mol^{-1}$.

**Computational Data on X−O Bond Dissociation Enthalpies.** The X−O bond dissociation enthalpy of several species was calculated according to the procedure described by Lee and Holm[13c] computing the enthalpy of reaction with molecular oxygen for several X/XO couples as shown in Scheme 1 (reaction (ii)). The X−O bond dissociation enthalpy corresponding to reaction (i) in Scheme 1 was then derived as BDE = $-\Delta H_{X/XO} + \Delta H^0_m(O(g))$, where $\Delta H^0_m(O(g)) = 59.55$ kcal $mol^{-1}$.[41]

Computed X−O bond dissociation enthalpies performed at the M05-2X/6-311G(3df,2p) and G3 level, together with experimental values, are collected in Table 2. G3 theory is known for

**Scheme 1. Thermodynamic Cycle Used to Obtain Computationally the BDE**

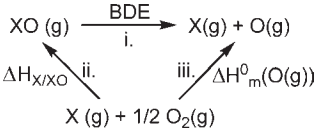


delivering chemical accuracy; however, its high computational cost most often give preference to the less computationally demanding DFT methods. Cundari and co-workers[42] have shown that the G3 method performs within the experimental error in calculating the thermochemistry of OAT reactions, while DFT methods such as the popular B3LYP functional provided inadequate results. As can be seen in Table 2, a good agreement between experimental data and calculated values at the M05-2X/6-311G(3df,2p) level is obtained for all the species studied. For the smallest molecules where the G3 methodology is applicable, similar results are obtained at the M05-2X/6-311G(3df,2p) level. Calculated values using the B3LYP functional give worse results as previously shown by Cundari and co-workers[42] giving the worst agreement with the experimental (or G3-calculated) data with the phosphines (Supporting Information, Table S1).

**Synthesis and Structure of SIPr·MesCNO.** As discussed earlier, we initially studied the reaction of SIPr and MesCNO in hopes of using this as an entry to measure enthalpies of OAT to NHC ligands forming cyclic ureas as shown in eq 8. OAT did not occur in spite of being thermochemically highly favorable (see Table 2), but simple binding of the SIPr to MesCNO as shown in reaction 11.

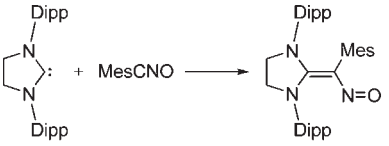


(11)

Dipp: 2,6-diisopropylphenyl

The crystal structure of the adduct shows binding between the lone pair of electrons of the NHC at the electrophilic C atom of MesCNO as shown in Figure 3.

This mode of binding resembles that to $CS_2$ which is displayed for both NHC and $R_3P$ ligands.[27a] Louie and co-workers[27b] have even reported adducts between $CO_2$ and NHCs. On the basis of the analogous Lewis basicity of NHCs and $R_3P$ compounds, the isolation and characterization of the adduct shown in Figure 3 suggested that attack of $R_3P$ at MesCNO might also proceed by initial attack at the C atom rather than the O atom and that this was the explanation of why it and not PyO is an efficient OAT reagent for phosphines. This prompted kinetic and computational study of the reaction mechanism of phosphines and MesCNO. Detailed synthetic and computational study of the adducts between a range of NHCs and MesCNO are in progress.[43]

**UV−vis Kinetic Study of Reaction of MesCNO with (Ar[$^t$Bu]N)$_3$MoP.** Kinetic analysis of the reaction of MesCNO with (Ar[$^t$Bu]N)$_3$MoP was performed on a UV−vis spectrophotometer under pseudo first order conditions with large excess of MesCNO in both $CH_2Cl_2$ and toluene solution. Time-resolved spectra show the appearance and growth of the peak at 550 nm that corresponds to the absorbance of independently prepared (Ar[$^t$Bu]N)$_3$MoPO. The exponential growth of this peak was used for kinetic analysis. Kinetic traces were fit to a single exponential function, and rate constants were obtained, $k_{obs} = k_1$[MesCNO] (Supporting Information, Figure S1).

**Table 2. BDEs (in kcal mol$^{-1}$) for the Reaction XO(g) → X(g) + O(g) Computed at the M05-2X/6-311G(3df,2p) and G3 Levels, and Compared to Experimental Data[a]**

| X | M05-2X/6-311G(3df,2p) | G3 | experimental[b] |
|---|---|---|---|
| NN | 38.0 [−2.0] | 40.8 [0.8] | 40.0 |
| PhCN | 48.5 | 50.0 | |
| MesCN | 48.1 [−4.2] | 48.8 [−3.5] | 52.3[c] |
| Py[d] | 61.7 [−1.6] | 63.6 [0.3] | 63.3 |
| NP | 74.6 | 78.3 | |
| THT[e] | 82.1 | 84.8 | |
| $Me_2S$ | 88.3 [1.7] | 86.0 [−0.6] | 86.6 |
| PP | 90.1 | 90.1 | |
| (Ar[$^t$Bu]N)$_3$MoP | 105.9 [−3.0][f] | | 108.9[g] |
| CO | 128.2 [1.0] | 128.7 [1.5] | 127.2 |
| $Ph_3P$ | 130.2 [−2.0] | | 132.2[g] |
| $Cy_3P$ | 135.3 [−2.3] | | 137.6[g] |
| $Me_3P$ | 133.0 [−5.5] | 134.9 [−3.6] | 138.5[g] |
| SIPr | 151.5 | | |

[a] $BDE_{calc}$ − $BDE_{exp}$ is shown in brackets beside the computed values. [b] Unless stated otherwise, values taken from ref 19. [c] Value taken from ref 18. [d] Pyridine. [e] Tetrahydrothiophene. [f] Using the Stuttgart-Dresden MWB28[38] effective core potential and basis including a set of additional f functions for Mo and the 6-311G(d,p) basis set for all other elements. [g] This work.

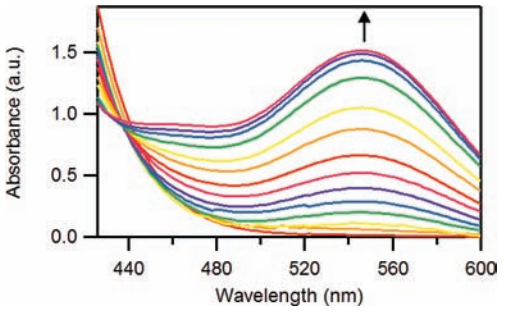


**Figure 1.** Spectral data as a function of time taken at 15 °C in $CH_2Cl_2$ with 25 mM MesCNO ([(Ar[$^t$Bu]N)$_3$MoP] = 0.6 mM), over a time interval of 60 min showing the rise in the band at 550 nm because of increase in [(Ar[$^t$Bu]N)$_3$MoPO].

Under high concentrations of MesCNO (100 mM), complete formation of (Ar[$^t$Bu]N)$_3$MoPO was followed by its slow partial decomposition, which could be seen as a minor decrease in the intensity of the peak at 550 nm and a slow appearance of a shoulder at 440 nm over longer periods of time (3−4 h, Figure 1). The minor decomposition was judged to not compromise kinetic analysis of the (Ar[$^t$Bu]N)$_3$MoPO formation step. The identity of the decomposition products was not established. Plots of $k_{obs}$ versus [MesCNO] gave straight lines as shown in Supporting Information, Figure S2, and were used to derive second-order rate constants in $CH_2Cl_2$: $k_{15\ °C} = 0.11\ M^{-1}\ s^{-1}$; $k_{22\ °C} = 0.15\ M^{-1}\ s^{-1}$; $k_{30\ °C} = 0.20\ M^{-1}\ s^{-1}$.

Identical kinetic experiments were repeated in toluene solution. Reaction rate as a function of temperature was measured with [MesCNO] = 50 mM and [(Ar[$^t$Bu]N)$_3$MoP] = 0.6 mM at


dx.doi.org/10.1021/ic2013599 |Inorg. Chem. 2011, 50, 9620–9630

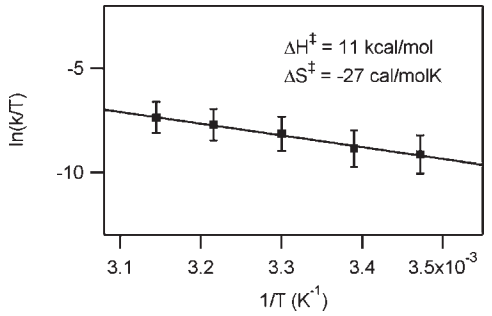


**Figure 2.** Eyring plot for reaction between MesCNO and $(Ar[^tBu]N)_3$-MoP in toluene.

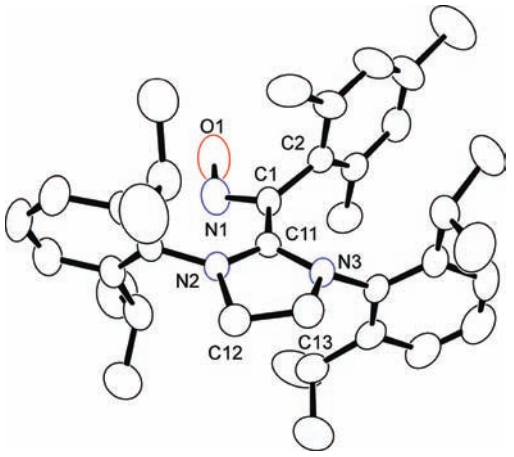


**Figure 3.** Thermal ellipsoid plot (40% probability) of the SIPr·MesCNO adduct. Selected distances (Å) and angles (deg): C1−C8, 1.521(4); C8−N2, 1.326(2); C10−N2, 1.451(2); N1−C1−C8−N2, 84.6. Complete structural data is available in Supporting Information.

five different temperatures: 15, 22, 30, 38, and 45 °C. In the replicate experiments for the same temperature in each solvent, $k_{obs}$ in $CH_2Cl_2$ and toluene were found to be similar as shown in the Supporting Information, Table S2. An Eyring plot was generated for the temperature dependence study in toluene solution, and activation parameters were calculated (Figure 2). The graphical analysis provided $\Delta H^{\ddagger} = 11$ kcal mol$^{-1}$ and $\Delta S^{\ddagger} = -27$ cal mol$^{-1}$ K$^{-1}$.

**FTIR Kinetic Studies of Reaction of MesCNO with $R_3P$, $(Ar[^tBu]N)_3MoP$ and SIPr.** To compare the rates of oxidation of tertiary phosphines to that of $(Ar[^tBu]N)_3MoP$, it was necessary to use vibrational spectroscopy because there is no observable color change when the phosphines are oxidized to the phosphine oxides because both are colorless. In addition, discovery of binding of SIPr to MesCNO was investigated kinetically for purposes of comparison of simple binding of the NHC to binding plus OAT which occurs for the phosphines and phosphide substrates. Reactions were run in a thermostatted FTIR cell under argon atmosphere at a balanced 1:1 ratio of [MesCNO]:[$R_3P$]. As a check, the kinetics of $(Ar[^tBu]N)_3MoP$ oxidation was also investigated by FTIR in toluene. A typical difference plot for oxidation of $(Ar[^tBu]N)_3MoP$ by MesCNO is shown in Supporting Information, Figure S3, and the linear second order plot derived from it in Supporting Information, Figure S4.

Attempts to detect intermediates in these reactions were not successful. Even at −40 °C, FTIR spectral data for the reaction of

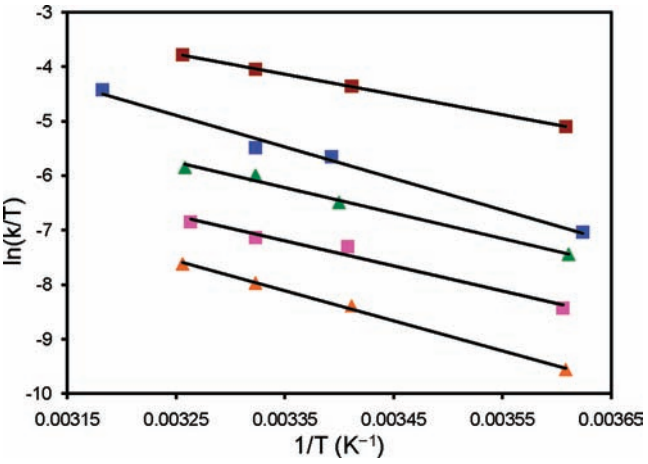


**Figure 4.** Eyring plots for reaction of MesCNO and SIPr (top line, brown square); $Me_3P$ (second line, blue squares), $Cy_3P$ (third line, green triangles), $(p\text{-tolyl})_3P$ (fourth line, pink square), and $(Ar[^tBu]N)_3MoP$ (bottom line, orange triangles).

**Table 3. Rate Constants at ≈20 °C and Derived Activation Parameters As Well As Reaction Enthalpies for Interaction between X and MesCNO**

| X | $k$ ($M^{-1}$ $s^{-1}$) | $\Delta H^{\ddagger}$ (kcal mol$^{-1}$) | $\Delta S^{\ddagger}$ (cal mol$^{-1}$ K$^{-1}$) | $\Delta H^0$ (kcal mol$^{-1}$) |
|---|---|---|---|---|
| $Me_3P$ | 1.0 | 11.5 | −19.5 | −86.2 |
| $Cy_3P$ | 0.45 | 9.3 | −28.4 | −85.3 |
| $(p\text{-tolyl})_3P$ | 0.20 | 9.1 | −30.9 | −79.9[a] |
| $(Ar[^tBu]N)_3MoP$[b] | 0.07 | 11.0 | −26.6 | −56.6 |
| $(Ar[^tBu]N)_3MoP$[c] | 0.04 | 11.0 | −27.0 | −56.6 |
| SIPR | 3.8 | 7.4 | −30.7 | |

[a] Refers to reaction of $Ph_3P$, expected to be similar to $(p\text{-tolyl})_3P$. [b] Values obtained by FTIR spectroscopy. [c] Values obtained by UV−vis spectrophotometry.

$Cy_3P$ and MesCNO displayed isosbestic points, and the rate of decay of MesCNO and the rate of buildup of $Cy_3PO$ were equal and opposite in sign. Eyring plots are shown in Figure 4; rate constants and activation parameters are shown in Table 3.

The entropies of activation are near −25 cal mol$^{-1}$ K$^{-1}$ in keeping with an associative transition state. The least unfavorable entropy of activation occurs, as might be expected, for $Me_3P$ since it is sterically the least hindered. The enthalpies of activation are in the range $\Delta H^{\ddagger} = 10 \pm 2$ kcal mol$^{-1}$, except for SIPr which involves only binding and not oxidative addition. The data determined by FTIR kinetics for $(Ar[^tBu]N)_3MoP$ are in good agreement with those determined independently by UV−vis studies. The rate and activation parameters in Table 3 appear in keeping with a common mechanism to these reactions.

**Theoretical Mechanism for Reaction of PhCNO and $Me_3P$.** Experimental work described above prompted theoretical investigation of OAT between $Me_3P$ and PhCNO as a model system. The reason OAT does not occur in the SIPr·MesCNO adduct is under computational study as part of a more detailed investigation of these adducts.[43] The frontier orbitals for $Me_3P$ and PhCNO calculated at the M05-2X/6-311G(3df,2p) level are shown in Figure 5. The shape of the orbitals suggests that a probable reaction pathway would involve attack of the highest


dx.doi.org/10.1021/ic2013599 |Inorg. Chem. 2011, 50, 9620–9630

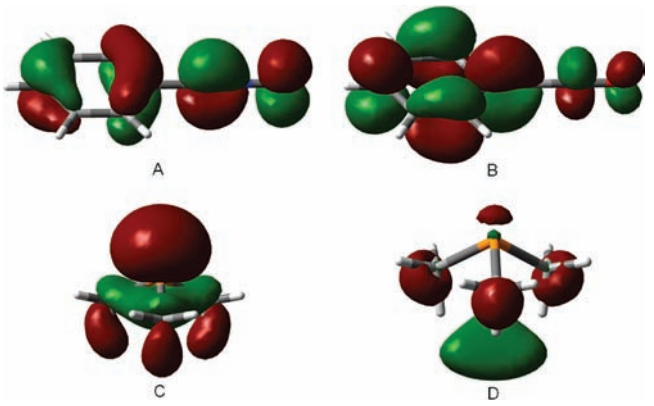


**Figure 5.** Computed frontier orbitals for $Me_3P$ and PhCNO. (A) HOMO of PhCNO; (B) LUMO of PhCNO; (C) HOMO of $Me_3P$; (D) LUMO of $Me_3P$.

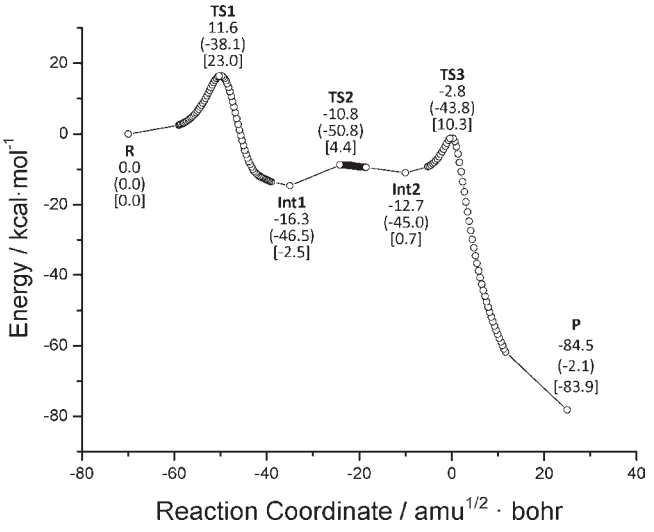


**Figure 6.** IRCs calculated at the M05-2X/6-311G(3df,2p) level. Relative enthalpies (in kcal $mol^{-1}$) (BSSE corrected), entropies between parentheses (in cal $mol^{-1}$ $K^{-1}$), and Gibbs energies between brackets (kcal $mol^{-1}$) at $T$ = 298 K.

occupied molecular orbital (HOMO) of $Me_3P$, which is essentially a lone pair orbital (C in Figure 5), to the lowest unoccupied molecular orbital (LUMO) of PhCNO (B in Figure 5), which is a delocalized $\pi^*$ orbital with a significant lobe on the C atom of PhCNO.

This is confirmed in the reaction mechanism obtained by computing the intrinsic reaction coordinate (IRC) at the same level of theory which is shown in Figure 6. The mechanism is composed of three consecutive stages, where three transition states have to be overcome, the first one assigned as the rate-limiting step. The structures of the computed transition states and intermediates are shown in Figure 7. Distances calculated at the M05-2X/6-311G(3df,2p) level for the reactants, products, transition states, and intermediates in Figure 6 are available in the Supporting Information, Table S3.

Several alternative mechanisms were also considered. Neither minima nor transition states were located corresponding to a 1,3-cycloaddition of PhNCO to $Me_3P$ according to a concerted mechanism. Likewise, direct OAT from PhNCO to $Me_3P$ was found to be repulsive and did not lead to reaction. A transition state higher in energy with a *syn* disposition of the $C_{ipso}-C-N-O$ moiety was also found (**TS1b**) which is shown in Supporting Information, Figure S5. This structure resembles that of the SIPr·MesCNO adduct shown in Figure 3. The lower energy of TS1 compared to TS1b can be attributed to electrostatic attraction between the positively charged P atom and the negatively charged O atom. Presumably steric forces do not allow this to be established for the SIPr·MesCNO adduct.[43]

**Reaction of the SIPr·MesCNO Adducts with $R_3P$, $(Ar[^tBu]N)_3$MoP, or $(Ar[^tBu]N)_3V$.** In view of the proposed mechanism of reaction of MesCNO with phosphines, it was of interest to see how blocking the electrophilic C atom of MesCNO in the SIPr·MesCNO adduct would affect its OAT reactivity. In that regard, it was important to first establish that the OAT ability of the SIPr·MesCNO adduct was not reduced significantly with respect to free MesCNO. Therefore, reactions 12 and 13 were investigated qualitatively.

$$(Ar[^tBu]N)_3V + MesCNO \rightarrow (Ar[^tBu]N)_3VO + MesCN \quad (12)$$

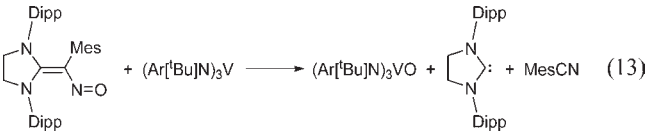


(13)

On the basis of visual observation, both reactions 12 and 13 occurred immediately upon mixing at room temperature. Stopped flow kinetic studies have shown that at room temperature, reaction of the adduct (reaction 13) is actually more rapid than OAT of MesCNO itself (reaction 12).[28] It is clear that no significant kinetic reduction in OAT ability through the O atom site occurred for the SIPr·MesCNO adduct compared to free MesCNO in its reaction with $(Ar[^tBu]N)_3V$. Thus it can be concluded that reaction of coordinatively unsaturated metal complexes with the SIPr·MesCNO adduct is not impaired by coordination of the NHC; in fact, it is slightly enhanced.[28]

In contrast, reactivity with $R_3P$ is shut down when an NHC coordinates and blocks the C atom binding site of MesCNO. Thus, reaction 14 did not proceed at room temperature over a four hour period.

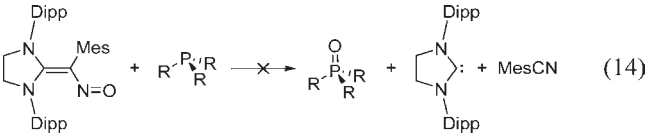


(14)

In a similar way $(Ar[^tBu]N)_3$MoP, which is efficiently oxidized by free MesCNO, undergoes no reaction with the SIPr·MesCNO adduct.

**Cases Where MesCNO Did Not Perform OAT.** In addition to the inability of MesCNO to oxidize the N-heterocyclic carbenes to form the corresponding cyclic ureas, several reactions that are thermodynamically favorable for OAT from MesCNO were found not to occur at room temperature in toluene solution. In spite of the fact that reaction 10 occurs, corresponding reaction of $(Ar[^tBu]N)_3$MoN as shown

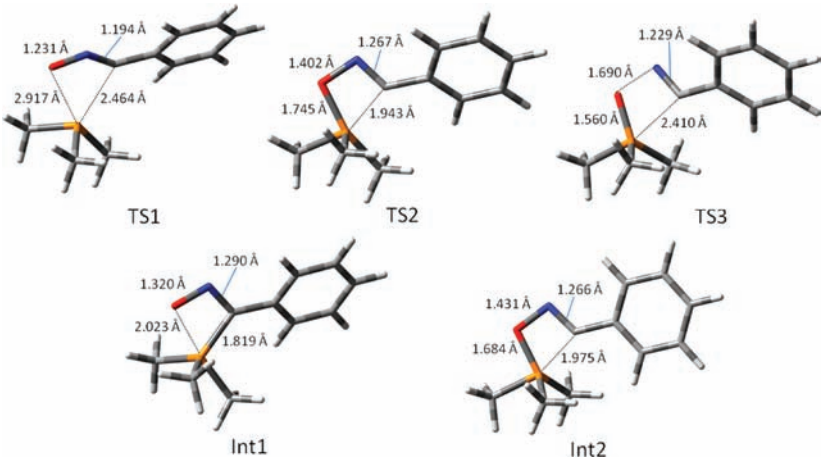


**Figure 7.** Computed structures of intermediates and transition states for reaction of $Me_3P$ and PhNCO at the M05-2X/6-311G(3df,2p) level. See Figure 5 for relative energies.

in reaction 15 was not observed.[44]

$$(Ar[^tBu]N)_3MoN + MesCNO \not\longrightarrow (Ar[^tBu]N)_3MoNO + MesCN \quad (15)$$

Oxidation of tetrahydrothiophene and of pyridine (reactions 16 and 17) did not occur over 4 h at room temperature.

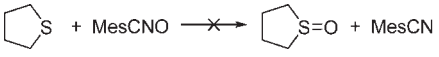


(16)


(17)

Attempts to oxidize dimethyl sulfoxide with MesCNO also showed no reaction at room temperature over several hours.

## DISCUSSION

MesCNO has proven to be a useful reagent for OAT to phosphines and phosphides for the systems shown in Table 1, and this work is now being extended to metal complexes.[28] OAT reactions of MesCNO can follow two different reaction channels: reaction with a Lewis acid may occur at the terminal O, but OAT reactions with a Lewis base may occur by attack at the electrophilic C atom. This second mechanistic possibility was envisioned only after stable adducts between NHC and MesCNO were discovered and shown to involve coordination of the nucleophilic carbene to the electrophilic C atom of MesCNO as shown in Figure 3. Since there is a strong similarity between NHCs and $R_3P$ in their coordination chemistry to metals,[45] this suggested that nonmetal oxidation by MesCNO may proceed through a similar adduct for the phosphine as that found to be stable for the NHC. The discussion focuses on two areas: (*i*) the thermochemistry of OAT and its implication for the Mo−P bond in $(Ar[^tBu]N)_3MoPO$, and (*ii*) the mechanism of OAT to phosphines and phosphides.

**Thermochemistry of OAT Reactions.** Much thermochemical data on organophosphines date back to work done in the 1950s to 1960s, and modern compilations of experimental data usually can be traced back to work done a half century ago. An exception to that is Domalski's determination by rotating bomb calorimetry of accurate data for $Ph_3P$ and $Ph_3PO$.[46] The data for $Ph_3P$ were found to differ by ≈5 kcal $mol^{-1}$ from work done by Mortimer using static bomb calorimetry.[47] Classic work in reaction calorimetry by Skinner and co-workers on enthalpies of reaction of trialkyl phosphines with $H_2O_2$ includes in its final paragraph the possibility that the oxidation reactions may not have been quantitative because of possible formation of trialkyl phosphine peroxides and concludes with the statement: *"In our opinion, the thermochemical results given here need independent verification, possibly by oxidation studies based on some other agent than hydrogen peroxide"*.[48] The value for the P═O BDE in $Ph_3PO$ determined in this work in toluene solution of 132.2 ± 3.0 kcal $mol^{-1}$ is in good agreement with the gas phase value of Domalski[9] of 135.4 ± 2.8 kcal $mol^{-1}$. The data for $Me_3P$ and $Cy_3P$ are also in reasonable agreement with values quoted for other trialkyl phosphines reported in the literature.[49] In addition, computed BDE values at the M05-2X/6-311G(3df,2p) level are in excellent agreement with experimental data as shown in Table 2.

It is of interest to compare the data in Table 1 for OAT to earlier data for SAT. Surprisingly, there is a smaller gap between $Ph_3P$ and $Cy_3P$ bonded to O than to S. This may be due to a greater significance of $\pi$ bonding in the P═O compared to P═S bond in $R_3PE$ (E = O, S). Thus, the weaker basicity of $Ph_3P$ compared to $Cy_3P$ may be compensated in its bonding to O by an increased $\pi$ bonding capacity in $Ph_3P$ which would be expected to be a poorer $\sigma$ donor but better $\pi$ acceptor than $Cy_3P$. For S, since $\pi$-bonding would be expected to be of less importance than for O, the difference between $Ph_3P$ and $Cy_3P$ would be greater since it is now dominated by the $\sigma$-donor ability of the phosphine.

The P═O BDE in $Me_3PO$ (138.5 kcal $mol^{-1}$) is similar to the fundamental P═O BDE (140.8 kcal $mol^{-1}$) for the gas phase diatomic molecule phosphorus monoxide. The enthalpy of OAT from MesCNO to $(Ar[^tBu]N)_3MoP$ is nearly 30 kcal $mol^{-1}$ lower than that for $Me_3P$ and yields a very low P−O BDE. Detailed discussion of why the P−O BDE in $(Ar[^tBu]N)_3MoPO$ is so low is not warranted beyond noting that upon loss of an O atom, the Mo complex has a stronger Mo−P bond (Mo−P BDE of −92.2 kcal $mol^{-1}$ in $(Ar[^tBu]N)_3MoP$ vs −60.2 kcal $mol^{-1}$ in $(Ar[^tBu]N)_3MoPO$, see below), whereas this does not happen in the case of phosphines. Furthermore, it was considered of interest to compare the data for $(Ar[^tBu]N)_3MoPO$ to P≡P═O and N≡P═O. Computational studies (see Table 2)


dx.doi.org/10.1021/ic2013599 |*Inorg. Chem.* 2011, 50, 9620–9630

**Scheme 2. Measured and Derived Enthalpies for the $(Ar[^tBu]N)_3MoEO$ (E = P, N)[a]**

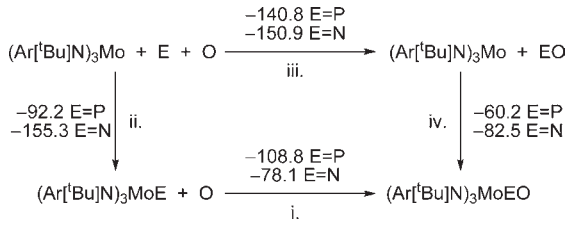


[a] All data in kcal $mol^{-1}$. For data relevant to $(Ar[^tBu]N)_3MoNO$ binding and the $(Ar[^tBu]N)_3MoN$ BDE see ref 52.

yielded the following values for the P−O bond dissociation enthalpy (kcal $mol^{-1}$): $(Ar[^tBu]N)_3MoPO$ [105.9], P≡P═O [90.1], and N≡P═O [78.3]. This trend appears to follow the expected decreasing basicity of the lone pair on P for $(Ar[^tBu]N)_3MoP$ versus P≡P versus N═P. Moreover, dissociation of an O atom from $(Ar[^tBu]N)_3MoPO$ forms $(Ar[^tBu]N)_3MoP$; dissociation of an O from PPO forms P≡P, and from NPO forms N≡P. Since it might reasonably be expected that the strongest triple bond in that series would be N≡P, then it seems reasonable the NPO would be more susceptible to O loss.

Since the enthalpy of formation of PO is known[50] the thermochemical data determined previously by us for the Mo−P bond in $(Ar[^tBu]N)_3MoP$[51] can be combined with the oxidation of $(Ar[^tBu]N)_3MoP$ to $(Ar[^tBu]N)_3MoPO$ reported here to calculate the enthalpy of coordination of PO to the $(Ar[^tBu]N)_3Mo$ fragment as shown in Scheme 2. Data are also included in Scheme 2 for N for comparison purposes.[52] The 60.2 kcal $mol^{-1}$ Mo−P BDE in $(Ar[^tBu]N)_3MoPO$ represents a strong metal−ligand bond but is still lower than the Mo−N BDE in $(Ar[^tBu]N)_3MoNO$ of 82.5 kcal $mol^{-1}$.

It is noteworthy that based on step (I) in Scheme 2, and a value of 59.5 kcal $mol^{-1}$ for step (III) of Scheme 1 that oxidation of $(Ar[^tBu]N)_3MoE$ by 1/2 $O_2$ to $(Ar[^tBu]N)_3MoEO$ is exothermic by 18.6 kcal $mol^{-1}$ for E = N, and 49.3 kcal $mol^{-1}$ for E = P. Thus, air oxidation of both the nitride and phosphide to the NO and PO complexes is thermodynamically favored. Oxidation of $(Ar[^tBu]N)_3MoN$ is not as favorable as for $(Ar[^tBu]N)_3MoP$ and this may be due to in part to the greater strength of the Mo≡N bond in $(Ar[^tBu]N)_3MoN$. The Mo−N distance in the nitride is shorter than in the nitrosyl complex. That is in keeping with the stronger Mo−N bond in $(Ar[^tBu]N)_3MoN$ (BDE= 155.3 kcal $mol^{-1}$) than that for $(Ar[^tBu]N)_3MoNO$ (BDE = 82.5 kcal $mol^{-1}$). However, as first pointed out by Cummins,[21] the Mo−P distance of 2.079 Å in $(Ar[^tBu]N)_3MoPO$ is 0.04 Å shorter than the Mo−P distance in $(Ar[^tBu]N)_3MoP$. This has led to speculation that the longer Mo−P bond in the phosphide may in fact be weaker than that in the $(Ar[^tBu]N)_3MoPO$ complex. Computations by Frenking and co-workers[53] are in agreement with the experimental bond distances, and they have also concluded that the Mo−P BDE in $(Ar[^tBu]N)_3MoPO$ is higher than that of $(Ar[^tBu]N)_3MoP$. That conclusion is at odds with the data in Scheme 2 where the Mo−P BDE is nevertheless 30 kcal $mol^{-1}$ higher in the phosphide than in $(Ar[^tBu]N)_3MoPO$ in spite of its longer distance. Bond length and bond strength do not always correlate with each other.[54] The BDE is the enthalpy of a homolysis reaction (eqs 18 and 19 for the Mo−P bonds in both species) and thus depends exclusively on the relative stability of reactant and product states.

$$(Ar[^tBu]N)_3MoP \xrightarrow[kcal\,mol^{-1}]{\Delta H = 92.2} (Ar[^tBu]N)_3Mo + P \quad (18)$$

$$(Ar[^tBu]N)_3MoPO \xrightarrow[kcal\,mol^{-1}]{\Delta H = 60.2} (Ar[^tBu]N)_3Mo + PO \quad (19)$$

The difference between the two BDEs is related to the fact that when $(Ar[^tBu]N)_3MoPO$ dissociates it produces the stable molecule PO. There is a large increase in the P−O BDE which follows that dissociation. Subtracting reaction 18 from reaction 19 yields reaction 20.

$$(Ar[^tBu]N)_3MoPO + P \xrightarrow[kcal\,mol^{-1}]{\Delta H = -32} (Ar[^tBu]N)_3MoP + PO \quad (20)$$

The difference in BDEs relates directly to the OAT value in reaction 20. The fact that PO has a stronger P−O Bond (BDE = 140.8 kcal $mol^{-1}$) than does $(Ar[^tBu]N)_3MoPO$ (BDE = 108.9 kcal $mol^{-1}$) accounts for the apparent discrepancy in bond length/BDE.

**Mechanism of OAT from MesCNO to Phosphines and Phosphides.** Computational studies suggest that attack by $Me_3P$ at the O atom of MesCNO leads to a repulsive surface. The computed mechanism entails a gradual rise in energy as the reactants approach each other at 4−5 Å to make an adduct between the Lewis basic lone pair of electrons on $Me_3P$, and the Lewis acid site at the electrophilic C atom of MesCNO. The first transition state (**TS1**) has the highest energy along the pathway in keeping with experimental failure to observe buildup of any intermediate adduct in the reaction by FTIR or UV−vis spectroscopic studies. The calculated values of $\Delta H^{\ddagger}$ = 11.6 kcal $mol^{-1}$ and $\Delta S^{\ddagger}$ = −38.1 cal $mol^{-1}$ $K^{-1}$ are in reasonable agreement with the experimental values determined by FTIR spectroscopy in Table 3. In the computed structure of **Int1**, corresponding to an adduct between $Me_3P$ and the C atom of MesCNO, there is an electrostatic interaction between the positive P atom (formal charge = +1) in the adduct and the O of the NO group (formal charge = −1). For $Me_3P$ steric hindrance to this configuration may be smaller than for bulkier phosphines. A shallow intermediate state (**TS2**) is computed along the second part of the reaction trajectory which corresponds to formation of what is approximately a cyclic structure in **Int2**. The enthalpy of activation for the last transition state (**TS3**) is $\Delta H^{\ddagger}$ = 9.9 kcal $mol^{-1}$ comparable to the energetic barrier in the first step; however, the entropy of activation is $\Delta S^{\ddagger}$ = 1.2 cal $mol^{-1}$ $K^{-1}$ making this step more favorable in terms of Gibbs energy. Full establishment of the P═O bond in $Me_3PO$ is a powerful driving force for this highly exothermic reaction which proceeds smoothly to completion. This pathway avoids the lone pair-lone pair repulsion that would be present if $R_3P$ underwent direct attack at the O atom of MesCNO. In this type of mechanism the C atom functions somewhat like a metal;[55] $R_3P$ coordinates and as a consequence of its electron donation develops a partial positive charge. The C atom gains electron density in this interaction, and this is delocalized to the O atom of MesCNO. It is noteworthy that blocking the C atom site by prior coordination of an NHC disrupts OAT activity for nonmetal but not for metal compounds

**Scheme 3. Oxidation of Nitrile Oxides by Amine Oxides**[a]

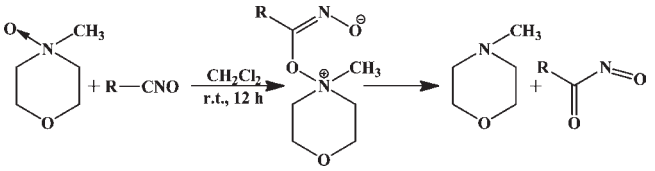


[a] See ref 56.

as shown in reactions 13 and 14. This provides support for two different mechanisms being operative in OAT with MesCNO.

There is literature precedent for the second proposed mechanism. Oxidation of nitrile oxides by amine oxides has been proposed to yield nitrosocarbonyls which may be trapped by dienes or other receptors.[56] The proposed first step in this reaction involves nucleophilic attack of the O of the amine oxide at the C of MesCNO to produce a zwitterionic intermediate which then dissociates as shown in Scheme 3. The central intermediate zwitterion proposed resembles the computed intermediate **Int1** in Figure 6.

Also of interest are the unsuccessful OAT reactions involving nonmetals that were surveyed here including tetrahydrothiophene, pyridine, and $(Ar[^tBu]N)_3MoN$. In spite of being computed to be exothermic in each case, for none of these combinations was OAT observed. An explanation is that for OAT to occur by the mechanism outlined here for nonmetals, the nucleophile must be strong enough to form a zwitterionic intermediate by nucleophilic attack at the C atom of MesCNO; however, it must also be capable of forming a cyclic intermediate by utilizing expanded valence. It seems plausible that $(Ar[^tBu]N)_3MoN$ and Py, even if they were to form an adduct at C with MesCNO similar to that observed in the reaction of MesCNO with NHCs, could not readily undergo valence expansion at the N atom beyond lone pair coordination. Tetrahydrothiophene may be capable of undergoing subsequent OAT chemistry via 1,3-cycloaddition but may not be basic enough to form an adduct with MesCNO. At this point, we have found only $R_3P$ and, somewhat surprisingly, $(Ar[^tBu]N)_3MoP$ capable of doing this.

## SUMMARY

Mesityl nitrile oxide is a versatile OAT reagent. Reactivity with coordinatively unsaturated metal complexes occurs rapidly through initial coordination of the terminal O atom. Oxidation of $R_3P$ and $(Ar[^tBu]N)_3MoP$ on the other hand occurs in minutes at room temperature but follows a different mechanism in which nucleophilic attack at the electrophilic C atom of MesCNO is followed by a cyclic transition state leading to OAT and elimination of MesCN. Reaction of MesCNO with $(Ar[^tBu]N)_3MoP$ provides ready entry to $(Ar[^tBu]N)_3MoPO$ which is a unique terminal phosphorus monoxide complex. However, the P−O BDE in this complex is some 30 kcal $mol^{-1}$ lower than in $R_3PO$ and corresponds more closely to computed values for PPO or NPO. In spite of the fact that the Mo−P bond in $(Ar[^tBu]N)_3MoPO$ is shorter than in $(Ar[^tBu]N)_3MoP$, the Mo−P BDE in $(Ar[^tBu]N)_3MoPO$ (60.2 kcal $mol^{-1}$) is lower than in $(Ar[^tBu]N)_3MoP$ (92.2 kcal $mol^{-1}$). This may be attributed to the fact that dissociation of PO results in an increase in the P−O bond strength for the free molecule compared to its adduct. Neither $(Ar[^tBu]N)_3MoN$, THT, nor Py are oxidized under the same conditions in which $R_3P$ oxidation is facile. It appears that two criteria exist for the OAT via this mechanism: (i) the reagent must be nucleophilic enough for adduct formation at the C atom, (ii) and it must be capable of expanded valence for a cyclic OAT transition state. Coordination of $R_3P$ appears to satisfy both these requirements. The novel remote site attack displayed here may be of utility in design of other reagents to achieve difficult OAT reactions to other nonmetal substrates. Additional synthetic, mechanistic, and thermochemical studies are in progress to expand understanding and utilization of OAT reactivity of nitrile oxides.

## ASSOCIATED CONTENT

**Supporting Information.** Spectroscopic, kinetic, structural, and computational data. This material is available free of charge via the Internet at http://pubs.acs.org.

## AUTHOR INFORMATION

**Corresponding Author**
*E-mail: c.hoff@miami.edu.

## ACKNOWLEDGMENT

Support of this work by the National Science Foundation Grants CHE 0615743 (CDH), 0750140 (ERA), 0724158 (CCC) and by the Spanish Ministry of Science and Innovation (MICINN) CTQ2009-07120 (M.T.) is gratefully acknowledged. M.T. and L.M.F. acknowledge MICINN for a "Juan de la Cierva" and a "Ramón y Cajal" contract. The authors wish to thank Jared S. Silvia (MIT) for a gift of $(Ar[^tBu]N)_3V$ and Alex T. Vai (MIT) for help in preparing $(Ar[^tBu]N)_3MoP$.

## REFERENCES

(1) Nam., W. *Acc. Chem. Res.* **2007**, *40*, 465. This is the first article in an issue dedicated to oxygen activation.

(2) Horváth, H. T.; Anastas, P. T. *Chem. Rev.* **2007**, *107*, 2167. This is the first article in an issue dedicated to green chemistry and containing several articles on green oxidation.

(3) (a) Parmon, V.; Panov, G.; Uriarte, A.; Noskov, A. *Catal. Today* **2005**, *100*, 115. (b) Hintz, P. A.; Sowa, M. B.; Ruatta, S. A.; Anderson, S. L. *J. Chem. Phys.* **1991**, *94*, 6446.

(4) (a) Vaughan, G. A.; Rupert, P. B.; Hillhouse, G. L. *J. Am. Chem. Soc.* **1987**, *109*, 5538. (b) Vaughan, G. A.; Hillhouse, G. L.; Lum, R. T.; Buchwald, S. L.; Rheingold, A. L. *J. Am. Chem. Soc.* **1988**, *110*, 7215. (c) Vaughan, G. A.; Sofield, C. D.; Hillhouse, G. L.; Rheingold, A. L. *J. Am. Chem. Soc.* **1989**, *111*, 5491. (d) Matsunaga, P. T.; Hillhouse, G. L.; Rheingold, A. L. *J. Am. Chem. Soc.* **1993**, *115*, 2075. (e) Koo, K.; Hillhouse, G. L.; Rheingold, A. L. *Organometallics* **1995**, *14*, 456. (f) Harrold, N. D.; Waterman, R.; Hillhouse, G. L.; Cundari, T. R. *J. Am. Chem. Soc.* **2009**, *131*, 12872.

(5) (a) Tuan, D. F.-T.; Hoffmann, R. *Inorg. Chem.* **1985**, *24*, 871. (b) Tuan, D. F.-T.; Reed, J. W.; Hoffmann, R. *THEOCHEM (J. Mol. Struct.)* **1991**, *232*, 111. (c) Armor, J. N.; Taube, H. *J. Am. Chem. Soc.* **1969**, *91*, 6874. (d) Armor, J. N.; Taube, H. *J. Am. Chem. Soc.* **1970**, *92*, 2560. (e) Armor, J. N.; Taube, H. *J. Chem. Soc. D* **1971**, 287. (f) Diamantis, A. A.; Sparrow, G. J. *J. Chem. Soc. D* **1969**, 469. (g) Diamantis, A. A.; Sparrow, G. J. *J. Chem. Soc. D* **1970**, 819. (h) Diamantis, A. A.; Sparrow, G. J. *J. Colloid Interface Sci.* **1974**, *47*, 455. (i) Diamantis, A.; Sparrow, G.; Snow, M.; Norman, T. *Aust. J. Chem.* **1975**, *28*, 1231. (j) Bottomley, F.; Crawford, J. R. *J. Chem. Soc. D* **1971**, 200. (k) Bottomley, F.; Crawford, J. R. *J. Am. Chem. Soc.* **1972**, *94*, 9092. (l) Bottomley, F.; Armor, J. N. *Inorg. Synth.* **1976**, 75. (m) Bottomley, F.; Brooks, W. V. F. *Inorg. Chem.* **1977**, *16*, 501.

(6) Piro, N. A.; Lichterman, M. F.; Harman, W. H.; Chang, C. J. *J. Am. Chem. Soc.* **2011**, *133*, 2108.
(7) (a) Otten, E.; Neu, R. C.; Stephan, D. W. *J. Am. Chem. Soc.* **2009**, *131*, 9918. (b) Neu, R. C.; Otten, E.; Stephan, D. W. *Angew. Chem., Int. Ed.* **2009**, *48*, 9709.
(8) Viege, A. S.; Slaughter, L. M.; Wolczanski, P. T.; Matsunaga, N.; Decker, S. A.; Cundari, T. R. *J. Am. Chem. Soc.* **2001**, *123*, 6419.
(9) Abu-Omar, M. M. In *Physical Inorganic Chemistry. Reactions, Processes, and Applications*; Bakac, A., Ed.; Wiley: Hoboken, NJ, 2010; p 75 and references cited therein.
(10) Cai, Y.; Ellern, A.; Espenson, J. H. *Inorg. Chem.* **2005**, *44*, 2560.
(11) Keith, J. M.; Tomil, Z. D.; Zaric, S. D.; Hall, M. B. *J. Mol. Catal. A: Chem.* **2010**, *324*, 15.
(12) Park, J.; Morimoto, Y.; Lee, Y. M.; Nam, W.; Fukuzumi, S. *J. Am. Chem. Soc.* **2011**, *133*, 5236.
(13) (a) Holm, R. H. *Chem. Rev.* **1987**, *87*, 1401. (b) Holm, R. H.; Donahue, J. P. *Polyhedron* **1993**, *12*, 571. (c) Lee, S. C.; Holm, R. H. *Inorg. Chim. Acta* **2008**, *361*, 1166.
(14) Grundmann, C.; Grünanger, P. *The nitrile oxides: versatile tools of theoretical and preparative chemistry*; Springer-Verlag: Berlin, Germany, 1971.
(15) Haaland, A. *Angew. Chem., Int. Ed. Engl.* **1989**, *28*, 992–1007.
(16) Shiro, M.; Yamakawa, M.; Kubota, T. *Acta Crystallogr., Sect. B: Struct. Sci.* **1979**, *35*, 712–716.
(17) Herzberg, G. *Electronic spectra and electronic structure of polyatomic molecules*; Van Nostrand: New York, 1966; p 1.
(18) Luo, Y. R. *Handbook of Bond Dissociation Energies in Organic Compounds*; CRC Press: Boca Raton, FL, 2003.
(19) The authors are not aware of this thermodynamically favored loss of $O_2$ occurring in either catalyzed or uncatalyzed reactions.
(20) (a) Grundmann, C.; Frommeld, H.-D. *J. Org. Chem.* **1965**, *30*, 2077. (b) Sicard, G.; Baceiredo, A.; Crocco, G.; Bertrand, G. *Angew. Chem., Int. Ed. Engl.* **1988**, *27*, 301.
(21) (a) Johnson, M. J. A.; Odom, A. L.; Cummins, C. C. *Chem. Commun.* **1997**, 1523–1524. (b) Piro, N. A.; Cummins, C. C. *J. Am. Chem. Soc.* **2009**, *131*, 8764–8765.
(22) Beck, W.; Keubler, M.; Leidl, E.; Nagel, U.; Schaal, M.; Cenini, S.; Buttero, P. D.; Licandro, E.; Maiorana, S.; Villa, A. C. *Chem. Commun.* **1981**, 446.
(23) Genco, N. A.; Partis, R. A.; Alper, H. *J. Org. Chem.* **1973**, *38*, 4365.
(24) Feuer, H., Ed.; *Nitrile Oxides, Nitrones, and Nitronates in Organic Synthesis*; John Wiley & Sons: Hoboken, NJ, 2008.
(25) (a) Bokach, N. A.; Khripoun, A. V.; Kukushkin, V. Y.; Haukka, M.; Pombeiro, A. J. L. *Inorg. Chem.* **2003**, *42*, 896. (b) Kuznetsov, M. L.; Kukushkin, V. Y.; Dement'ev, A. I.; Pombeiro, A. J. L. *J. Phys. Chem. A* **2003**, *107*, 6108.
(26) (a) McDonough, J. E.; Mendiratta, A.; Curley, J. J.; Fortman, G. C.; Fantasia, S.; Cummins, C. C.; Rybak-Akimova, E. V.; Nolan, S. P.; Hoff, C. D. *Inorg. Chem.* **2008**, *47*, 2133. (b) Huang, J.; Schanz, H. J.; Stevens, E. D.; Nolan, S. P.; Capps, K. B.; Bauer, A.; Hoff, C. D. *Inorg. Chem.* **2000**, *39*, 1042. (c) Capps, K. B.; Wixmerten, B.; Bauer, A.; Hoff, C. D. *Inorg. Chem.* **1998**, *37*, 2861.
(27) (a) Delaude, L.; Demonceau, A.; Wouters, J. *Eur. J. Inorg. Chem.* **2009**, 1882–1891. (b) Duong, H. A.; Tekavec, T. N.; Arif, A. M.; Louie, J. *Chem. Commun.* **2004**, 112–113.
(28) Rybak-Akimova, E. V.; Palluccio, T.; Silvia, J. S.; Cummins, C. C.; Temprado, M.; Majumdar, S.; Cai, X.; Hoff, C. D., *work in progress*.
(29) Pangborn, A. B.; Giardello, M. A.; Grubbs, R. H.; Rosen, R. K.; Timmers, F. J. *Organometallics* **1996**, *15*, 1518.
(30) For a description see supporting information files in: Barybin, M. V.; Diaconescu, P. L.; Cummins, C. C. *Inorg. Chem.* **2001**, *40*, 2892 which presents a modified preparation from the original. Grundmann, C.; Dean, J. M. *J. Org. Chem.* **1965**, *30*, 2809.
(31) *Apex2 Version 2.2−0 and SAINT+ Version 7.46A*; Bruker Analytical X-ray System, Inc.: Madison, WI, 2007.
(32) (a) Sheldrick, G. M. *SHELXTL*, Version 6.1; Bruker Analytical X-ray Systems, Inc.: Madison, WI, 2000. (b) Sheldrick, G. M. *Acta Crystallogr.* **2008**, *A64*, 112–122.
(33) Becke, A. D. *J. Chem. Phys.* **1993**, *98*, 5648.
(34) Lee, C.; Yang, W.; Parr, R. G. *Phys. Rev. B* **1988**, *37*, 785.
(35) Zhao, Y.; Schultz, N. E.; Truhlar, D. G. *J. Chem. Theory Comput.* **2006**, *2*, 364.
(36) Frisch, M. J.; et al. *Gaussian 09*, revision B.01; Gaussian, Inc.: Wallingford, CT, 2010.
(37) (a) Simon, S.; Duran, M.; Dannenberg, J. J. *J. Chem. Phys.* **1996**, *105*, 11024. (b) Boys, S. F.; Bernardi, F. *Mol. Phys.* **1970**, *19*, 553.
(38) Andrae, D.; Haeussermann, U.; Dolg, M.; Stoll, H.; Preuss, H. *Theor. Chim. Acta* **1990**, *77*, 123.
(39) (a) Fukui, K. *Acc. Chem. Res.* **1981**, *14*, 363. (b) Hratchian, H. P.; Schlegel, H. B. *J. Chem. Theory Comput.* **2005**, *1*, 61.
(40) Curtiss, L. A.; Raghavachari, K.; Redfern, P. C.; Rassolov, V.; Pople, J. A. *J. Chem. Phys.* **1998**, *109*, 7764.
(41) Cox, J. D.; Wagman, D. D.; Medvedev, V. A. *CODATA Key Values for Thermodynamics*; Hemisphere: New York, 1989.
(42) Dinescu, A.; Whiteley, C.; Combs, R. R.; Cundari, T. R. *J. Phys. Chem. A* **2006**, *110*, 4053.
(43) Temprado, M.; Cai, X.; Majumdar, S.; Captain, B.; Hoff, C. D.; *work in progress*.
(44) Examples of nitride to NO conversion via OAT have been reported in the literature: Williams, D. S.; Meyer, T. J.; White, P. S. *J. Am. Chem. Soc.* **1995**, *117*, 823.
(45) Díez-González, S.; Marion, N.; Nolan, S. P. *Chem. Rev.* **2009**, *109*, 3612.
(46) Kirklin, D. R.; Domalski, E. S. *J. Chem. Thermodyn.* **1988**, *20*, 754.
(47) Bedford, A. F.; Mortimer, C. T. *J. Chem. Soc.* **1960**, 1622.
(48) Chernick, C. L.; Skinner, H. A. *J. Chem. Soc.* **1956**, 1401.
(49) The P−O BDEs for $Me_3PO$ from ref 19 of 139 kcal $mol^{-1}$ and for $Bu_3PO$ from ref 10 of 137.2 kcal $mol^{-1}$ are in agreement with the values of 138.5 and 137.6 kcal $mol^{-1}$ respectively for $Me_3PO$ and $Cy_3PO$ in this work.
(50) Data taken from the NIST Webbook. http://webbook.nist.gov/chemistry
(51) Stephens, F. H.; Johnson, M. J. A.; Diaconescu, P. L.; Cummins, C. C.; Kryatova, O. P.; Rybak-Akimova, E. V.; McDonough, J. E.; Hoff, C. D. *J. Am. Chem. Soc.* **2005**, *127*, 15191.
(52) Johnson, A. R.; Baraldo, L. M.; Cherry, J. P. F.; Tsai, Y. C.; Cummins, C. C.; Kryatov, S. V.; Rybak Akimova, V.; Capps, K. B.; Hoff, C. D.; Haar, C. M.; Nolan, S. P. *J. Am. Chem. Soc.* **2001**, *123*, 7271.
(53) Caramori, G. F.; Frenking, G. *Theor. Chem. Acc.* **2008**, *120*, 351.
(54) (a) Frenking, G.; Wichmann, K.; Fröhlich, N.; Grobe, J.; Golla, W.; Le Van, D.; Krebs, B.; Läge, M. *Organometallics* **2002**, *21*, 2921. (b) Fischer, R. A.; Schulte, M. M.; Weiß, J.; Zsolnai, L.; Jacobi, A.; Huttner, G.; Frenking, G.; Boehme, C.; Vyboishckikov, S. F. *J. Am. Chem. Soc.* **1998**, *120*, 1237.
(55) Several recent articles have compared carbenes to metals, see: Martin, D.; Soleihavoup, M.; Bertrand, G. *Chem. Sci.* **2011**, *2*, 389.
(56) Quadrelli, P.; Mella, M.; Invernizzi, A. G.; Caramella, P. *Tetrahedron* **1999**, *55*, 10497.

## NOTE ADDED AFTER ASAP PUBLICATION

This paper was published on the Web on August 29, 2011, with a minor error in equation 4. The corrected version was reposted on September 1, 2011.